Int. J. Solids Structures Vol. 29, No. 19, pp. 2403–2419, 1992
Printed in Great Britain.

0020–7683/92 $5.00+.00

CIRCULAR INCLUSION PROBLEM IN ANTIPLANE PIEZOELECTRICITY

Y. EUGENE PAK
Grumman Corporate Research Center, Bethpage, NY 11714, U.S.A.

(*Received* 18 *August* 1991; *in revised form* 19 *December* 1991)

Abstract—A circular piezoelectric inclusion embedded in an infinite piezoelectric matrix is analysed in the framework of linear piezoelectricity. A closed-form solution is obtained for the case of a far-field antiplane mechanical load and a far-field inplane electrical load. It is shown that in modeling cavities, imposing an impermeable boundary condition is a good approximation provided that the piezoelectric material has high dielectric constant and strong electro–elastic coupling. Stress and electric field concentrations are also studied. It is shown that a high electric field can be induced in the inclusion under a mechanical load when the matrix and the inclusion are poled in the opposite directions. The path-independent M-integral of elastostatics, generalized to take piezoelectric effect into account, is used to study the energetics of a self-similarly expanding piezoelectric inclusion.

INTRODUCTION

Due to their intrinsic electro-mechanical coupling behavior, piezoelectric materials, particularly piezoelectric ceramics, have recently been widely used as actuators and sensors in "smart" materials and structures technology. This paper constitutes a continuing study in understanding the macroscopic behavior of these materials in the presence of defects such as cracks, dislocations, cavities and inclusions subjected to mechanical and electrical loads (Parton, 1976; Deeg, 1980; Zhou *et al.*, 1986; Shintani and Minagawa, 1988; Pak, 1990a,b; Shindo and Ozawa, 1990; Sosa, 1991; Suo, 1991; Wang, 1992). Commonly used piezoelectric materials are ceramics such as lead zirconate titanate (PZT), which are manufactured through conventional ceramic processing. These ceramics are then subjected to a poling process (application of strong electric field) that induces piezoelectricity and anisotropy in the material. The resulting anisotropy can be characterized as transversely isotropic with the poling direction normal to the isotropic plane. Bleustein (1968) analysed the antiplane piezoelectric dynamics problem and discovered the existence of Bleustein waves. He has shown that if one takes the plane normal to the poling direction as the plane of interest, only the out-of-plane mechanical deformations couple with the inplane electrical fields. This reduces the problem considerably to a simple potential problem for decoupled out-of-plane displacement, $u_z(x, y)$, and inplane electric potential, $\phi(x, y)$. The elastic fields and the electrical fields are coupled only through the constitutive equations.

The present work was largely motivated by the need to clarify some of the assumptions made in applying an electrical boundary condition at the interface between the internal cavity and the surrounding piezoelectric material. In solving previous piezoelectric boundary value problems, Pak (1990a) used a heuristic physical argument—that a drastic change in the dielectric constants (about three order of magnitude) occurs across the boundary between the cavity and the piezoelectric material—in justifying the electric impermeability condition at the interface. This rendered possible the decoupling of the domains occupied by the cavity and the piezoelectric material in the mathematical model, which significantly simplified the problem by allowing only the domain occupied by the piezoelectric material to be modeled. This is analogous to a thermoelasticity problem in which a heat insulation boundary condition is assumed to hold on the crack faces or at the rim of a hole. In this study, such restrictions will be lifted by modeling the electric field inside the hole (vacuum) as well as in the material. Furthermore, we will consider a more general case by introducing

a piezoelectric inclusion which, in the limiting case of vanishing elastic and piezoelectric constants, becomes a permeable hole containing free space with electric fields. Invoking governing equations of piezoelectricity with proper continuity conditions, a fully coupled two-domain piezoelectric inclusion-matrix problem can be formulated and solved. By examining the permeable-boundary solution, we can determine the conditions under which the use of impermeable boundary conditions is justified.

This analysis also enables us to examine the stress and electric field concentrations due to the presence of an inclusion. This study is useful in designing piezoelectric composites and in understanding the effects of second-phase particles and voids in piezoelectric materials. The understanding of electric field concentration can be useful in reducing the problem of dielectric breakdowns that frequently occur during a poling process. The path-independent M-integral will be used to study the energetics of a self-similarly growing circular inclusion (or a cavity) in the presence of both mechanical and electrical loads. This may be helpful in understanding thermodynamic forces that govern microstructural evolution and phase transformations in ferroelectric crystals.

During the course of this work, the author discovered that the boundary value problem considered in this paper has been solved by an alternate method (Honein *et al.*, 1990). However, the emphasis of this work is not on demonstrating a novel and elegant method of solving boundary value problems but rather on the understanding of interesting electro-elastic coupling behaviors that have not been studied previously.

PIEZOELECTRIC INCLUSION PROBLEM

Consider an infinitely long circular piezoelectric inclusion with a radius a embedded in another piezoelectric material, as shown in Fig. 1. The matrix and the inclusion are assumed to have different material properties, but they are assumed to have the same material orientation in that they have both been poled along the z-direction. The matrix, assumed to be infinite in all directions, is subjected to a far-field antiplane shear, $\sigma_{zy} = \tau_\infty$, and a far-field inplane electric field, $E_y = E_\infty$. A uniform electric field can be induced in a homogeneous piezoelectric material by applying a constant potential jump across the specimen. In the configuration shown in Fig. 1, only the out-of-plane displacement, u_z, couples with the inplane electric fields, E_r and E_θ. Therefore, if we only consider the out-of-plane displacement and the in-plane electric fields such that

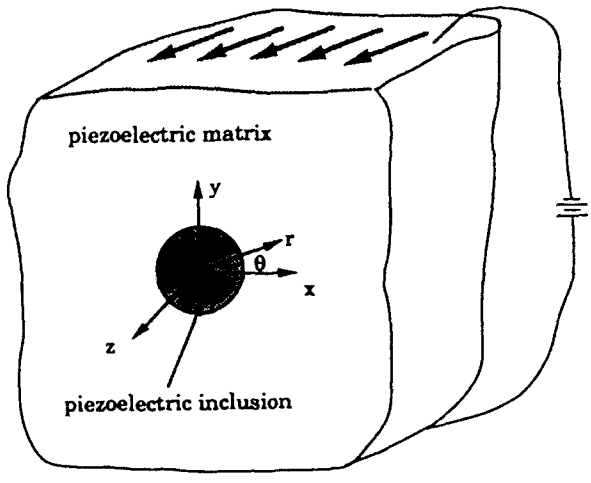

Fig. 1. Piezoelectric inclusion subjected to far-field antiplane shear and inplane electric field.

$$u_r^{(i)} = u_\theta^{(i)} = 0, \quad u_z^{(i)} = u_z^{(i)}(r,\theta), \quad E_r^{(i)} = E_r^{(i)}(r,\theta), \quad E_\theta^{(i)} = E_\theta^{(i)}(r,\theta), \quad E_z^{(i)} = 0, \quad (i = \mathrm{M}, \mathrm{I}), \tag{1}$$

the governing equations (Appendix A), in the absence of body forces and body charges, decouple and simplify to

$$\nabla^2 u_z^{(i)} = 0, \quad \nabla^2 \phi^{(i)} = 0, \quad (i = \mathrm{M}, \mathrm{I}), \tag{2}$$

where ∇^2 is the two-dimensional Laplacian operator

$$\nabla^2 \equiv \frac{\partial^2}{\partial r^2} + \frac{1}{r}\frac{\partial}{\partial r} + \frac{1}{r^2}\frac{\partial^2}{\partial \theta^2}, \tag{3}$$

and the superscripts M and I refer to the quantities in the matrix and the inclusion, respectively. The coupling between the elastic fields and the electrical fields occurs only through the constitutive equations (Appendix B)

$$\begin{aligned} \sigma_{zr}^{(i)} &= c_{44}^{(i)}\gamma_{zr}^{(i)} - e_{15}^{(i)}E_r^{(i)}, \quad \sigma_{z\theta}^{(i)} = c_{44}^{(i)}\gamma_{z\theta}^{(i)} - e_{15}^{(i)}E_\theta^{(i)} \\ D_r^{(i)} &= e_{15}^{(i)}\gamma_{zr}^{(i)} + \varepsilon_{11}^{(i)}E_r^{(i)}, \quad D_\theta^{(i)} = e_{15}^{(i)}\gamma_{z\theta}^{(i)} + \varepsilon_{11}^{(i)}E_\theta^{(i)}, \quad (i = \mathrm{M}, \mathrm{I}), \end{aligned} \tag{4}$$

where $\gamma_{ij}^{(i)}$ and $E_i^{(i)}$ are respectively the antiplane shear strains and inplane electric fields, which are defined as

$$\gamma_{zr}^{(i)} = \frac{\partial u_z^{(i)}}{\partial r}, \quad \gamma_{z\theta}^{(i)} = \frac{1}{r}\frac{\partial u_z^{(i)}}{\partial \theta}, \quad E_r^{(i)} = -\frac{\partial \phi^{(i)}}{\partial r}, \quad E_\theta^{(i)} = -\frac{1}{r}\frac{\partial \phi^{(i)}}{\partial \theta}, \quad (i = \mathrm{M}, \mathrm{I}). \tag{5}$$

We can obtain the solution to this problem by first expressing the independent variables in series.

In the matrix,

$$u_z^{\mathrm{M}}(r,\theta) = \sum_{n=1}^{\infty} [a_n r^n + b_n r^{-n}] \sin n\theta, \quad \phi^{\mathrm{M}}(r,\theta) = \sum_{n=1}^{\infty} [c_n r^n + d_n r^{-n}] \sin n\theta. \tag{6}$$

In the inclusion,

$$u_z^{\mathrm{I}}(r,\theta) = \sum_{n=1}^{\infty} f_n r^n \sin n\theta, \quad \phi^{\mathrm{I}}(r,\theta) = \sum_{n=1}^{\infty} g_n r^n \sin n\theta, \tag{7}$$

where a_n, b_n, c_n, d_n, f_n and g_n are constant coefficients that are to be determined from the far-field conditions

$$\left.\begin{aligned} \sigma_{zy}^{\mathrm{M}} &= \tau_\infty \\ E_y^{\mathrm{M}} &= E_\infty \end{aligned}\right\} \quad \text{as } r \to \infty, \tag{8}$$

and the continuity conditions across the matrix-inclusion interface

$$\left.\begin{aligned} u_z^{\mathrm{M}} &= u_z^{\mathrm{I}} \\ \sigma_{zr}^{\mathrm{M}} &= \sigma_{zr}^{\mathrm{I}} \\ \phi^{\mathrm{M}} &= \phi^{\mathrm{I}} \\ D_r^{\mathrm{M}} &= D_r^{\mathrm{I}} \end{aligned}\right\} \quad \text{at } r = a. \tag{9}$$

The solution is obtained by solving a system of six algebraic equations arising from the conditions given in (8) and (9).

In the matrix,

$$u_z^M = \left[a_1 r + \frac{b_1}{r}\right]\sin\theta, \quad \phi^M = \left[c_1 r + \frac{d_1}{r}\right]\sin\theta, \quad \gamma_{zr}^M = \left[a_1 - \frac{b_1}{r^2}\right]\sin\theta$$

$$\gamma_{z\theta}^M = \left[a_1 + \frac{b_1}{r^2}\right]\cos\theta, \quad E_r^M = -\left[c_1 - \frac{d_1}{r^2}\right]\sin\theta, \quad E_\theta^M = -\left[c_1 + \frac{d_1}{r^2}\right]\cos\theta$$

$$\sigma_{zr}^M = \left[c_{44}^M a_1 + e_{15}^M c_1 - \frac{c_{44}^M b_1 + e_{15}^M d_1}{r^2}\right]\sin\theta, \quad \sigma_{z\theta}^M = \left[c_{44}^M a_1 + e_{15}^M c_1 + \frac{c_{44}^M b_1 + e_{15}^M d_1}{r^2}\right]\cos\theta$$

$$D_r^M = \left[e_{15}^M a_1 - \varepsilon_{11}^M c_1 - \frac{e_{15}^M b_1 - \varepsilon_{11}^M d_1}{r^2}\right]\sin\theta, \quad D_\theta^M = \left[e_{15}^M a_1 - \varepsilon_{11}^M c_1 + \frac{e_{15}^M b_1 - \varepsilon_{11}^M d_1}{r^2}\right]\cos\theta. \tag{10}$$

In the inclusion,

$$u_z^I = f_1 r\sin\theta, \quad \phi^I = g_1 r\sin\theta, \quad \gamma_{zr}^I = f_1\sin\theta, \quad \gamma_{z\theta}^I = f_1\cos\theta$$

$$E_r^I = -g_1\sin\theta, \quad E_\theta^I = -g_1\cos\theta, \quad \sigma_{zr}^I = [c_{44}^I f_1 + e_{15}^I g_1]\sin\theta, \quad \sigma_{z\theta}^I = [c_{44}^I f_1 + e_{15}^I g_1]\cos\theta$$

$$D_r^I = [e_{15}^I f_1 - \varepsilon_{11}^I g_1]\sin\theta, \quad D_\theta^I = [e_{15}^I f_1 - \varepsilon_{11}^I g_1]\cos\theta, \tag{11}$$

where

$$a_1 = \frac{\tau_\infty + e_{15}^M E_\infty}{c_{44}^M}, \quad c_1 = -E_\infty$$

$$b_1 = \frac{a^2\{a_1[c_{15}^{M2} - e_{15}^{I2} + (c_{44}^M - c_{44}^I)(\varepsilon_{11}^M + \varepsilon_{11}^I)] + 2c_1[e_{15}^M\varepsilon_{11}^I - e_{15}^I\varepsilon_{11}^M]\}}{\Delta}$$

$$d_1 = \frac{a^2\{2a_1[c_{44}^M e_{15}^I - c_{44}^I e_{15}^M] + c_1[(c_{44}^M + c_{44}^I)(\varepsilon_{11}^M - \varepsilon_{11}^I) + (e_{15}^M)^2 - (e_{15}^I)^2]\}}{\Delta}$$

$$f_1 = \frac{2\{a_1[c_{44}^M(\varepsilon_{11}^M + \varepsilon_{11}^I) + e_{15}^M(e_{15}^M + e_{15}^I)] + c_1[e_{15}^M\varepsilon_{11}^I - e_{15}^I\varepsilon_{11}^M]\}}{\Delta}$$

$$g_1 = \frac{2\{a_1[c_{44}^M e_{15}^I - c_{44}^I e_{15}^M] + c_1[(c_{44}^M + c_{44}^I)\varepsilon_{11}^M + e_{15}^M(e_{15}^M + e_{15}^I)]\}}{\Delta}$$

$$\Delta = (c_{44}^M + c_{44}^I)(\varepsilon_{11}^M + \varepsilon_{11}^I) + (e_{15}^M + e_{15}^I)^2. \tag{12}$$

As is well known in elastostatics and electrostatics, the strain and the electric field are constant in the inclusion. In the absence of mechanical fields, these solutions reduce to the classical electrostatic solution presented, for example, in Fano *et al.* (1960). In the absence of electrical fields, on the other hand, these solutions reduce to the classical antiplane elastostatic inclusion problem. Contours of constant electric potential and constant σ_{zy} stress are plotted in Figs 2(a, b), respectively.

ELECTRICAL BOUNDARY CONDITION

Unlike elastic fields, electric fields can permeate through vacuum and can exist inside the cavity of a dielectric or a piezoelectric material. This requires modeling of electric fields even in the absence of material inside the cavity. However, by carefully considering the interactions that take place at the interface, and by taking advantage of the fact that the piezoelectric materials have high dielectric constants and strong electro–elastic coupling, one can circumvent modeling the electric fields inside the cavity by imposing an impermeability condition on the boundary. The continuity of the normal component of electric displacement and the traction-free boundary condition require the following relations to hold on the boundary at $r = a$:

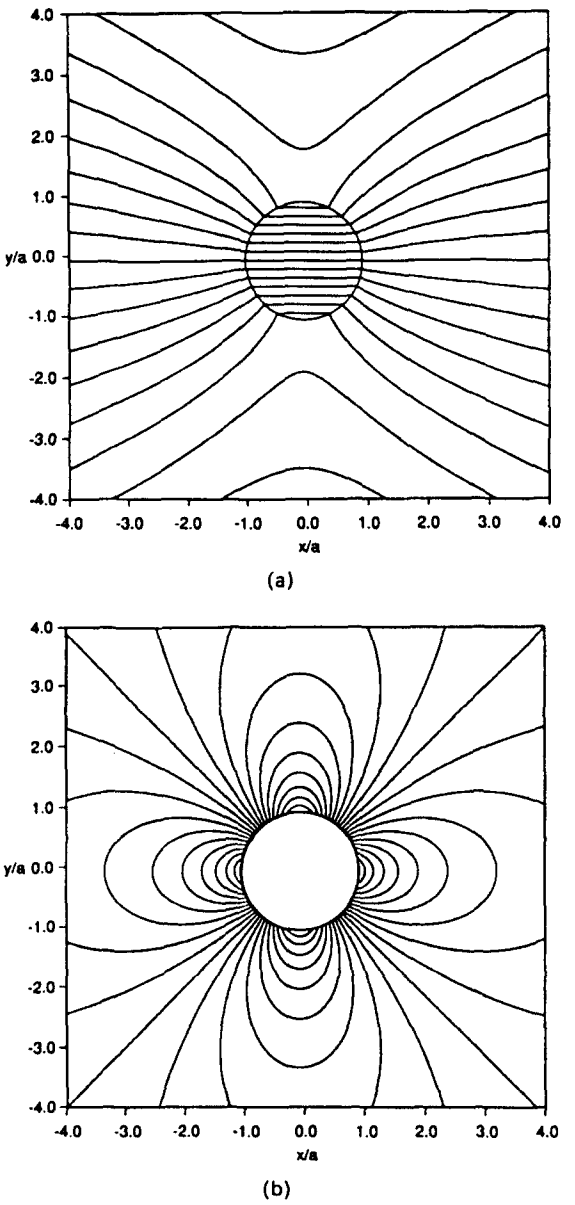

Fig. 2. Contours of constant (a) electric potential ϕ, (b) shear stress σ_{zy}.

$$e_{15}^{M}\gamma_{zr}^{M}+\varepsilon_{11}^{M}E_{r}^{M}=\varepsilon_{0}E_{r}^{I},\quad c_{44}^{M}\gamma_{zr}^{M}-e_{15}^{M}E_{r}^{M}=0. \tag{13}$$

We are letting ε_{11}^{I} be the same as ε_0, the permittivity of free space, since the cavity is assumed to be "filled" with vacuum. Solving for the ratio of the electric fields just inside and outside the permeable hole, we obtain

$$\left.\frac{E_{r}^{M}}{E_{r}^{I}}\right|_{r=a}=\frac{\varepsilon_{0}}{\varepsilon_{11}^{M}+e_{15}^{M2}/c_{44}^{M}}. \tag{14}$$

Substituting typical values for PZT ceramic (Appendix C), we find that

$$\left.\frac{E_{r}^{M}}{E_{r}^{I}}\right|_{r=a}\approx 3.8\times 10^{-4}\ll 1. \tag{15}$$

If we assume that E_r^I is of the same order of magnitude as E_∞, we can make an approximation

that $E_r^M|_{r=a} \cong 0$. This enables us to impose $D_r^M|_{r=a} = 0$ (since $\gamma_{rr}^M|_{r=a} = 0$ from the traction-free condition) and ignore the field inside the hole. We remind the reader that the expression given in eqn (14) has been derived solely from the boundary and continuity conditions and not from the solution to the boundary value problem. Therefore, we can ascertain only the relative magnitudes of the normal components of the electric field at the boundary. In order to show that the absolute value of $E_r^M|_{r=a}$ is small, i.e. $E_r^M|_{r=a} \ll E_\infty$, we need the solution to the permeable hole problem. This can be obtained from the piezoelectric inclusion solution by letting $c_{44}^I = e_{15}^I = 0$. Using the permeable hole solution, we arrive at

$$\frac{E_r^M|_{r=a}}{E_\infty} = \frac{2\varepsilon_0}{\varepsilon_{11}^M + \varepsilon_0 + (e_{15}^M)^2/c_{44}^M} \sin\theta \sim 7.6 \times 10^{-4} \ll 1. \tag{16}$$

We can now state that for typical piezoceramics, E_r^M is indeed very small compared to E_∞. This expression indicates, as does eqn (14), that there are two independent reasons for the normal component of an electric field to be negligibly small just inside the piezoelectric material at the boundary of a cavity, namely, (1) a high relative dielectric constant, $\varepsilon_{11}^M/\varepsilon_0 \gg 1$, and (2) a strong piezoelectric coupling, $(e_{15}^M)^2/(\varepsilon_0 c_{44}^M) \gg 1$. This point is clearly illustrated in Fig. 3. We can conclude from this study that in electro–elastic modeling of piezoelectric materials, one can impose $\mathbf{D} \cdot \mathbf{n} = 0$ on the cavity boundary without introducing serious errors, provided that the material has a high dielectric constant and strong piezoelectric coupling. There exists, however, an electric field inside the cavity, which is about twice the applied electric field. This jump in the normal component of the electric field across the cavity–matrix interface is due to the existence of bound surface polarization charges. One should exercise care in applying the $\mathbf{D} \cdot \mathbf{n} = 0$ condition on a very slender cavity (such as a crack) in electrostrictive materials. Readers are referred to McMeeking (1989) for a detailed discussion.

STRESS AND ELECTRIC FIELD CONCENTRATIONS

Equations (10) show that the maximum stress in the matrix can occur at $\theta = 0$ or at $\theta = \pi/2$, depending on the sign of the $(c_{44}^M b_1 + e_{15}^M d_1)$ term. It is clear from examining the expressions for b_1 and d_1 that this depends on various material parameters and should be determined case by case. Likewise, the maximum electric field in the matrix is determined by the sign of the d_1 term. At the same time, all the elastic and electrical fields are constant

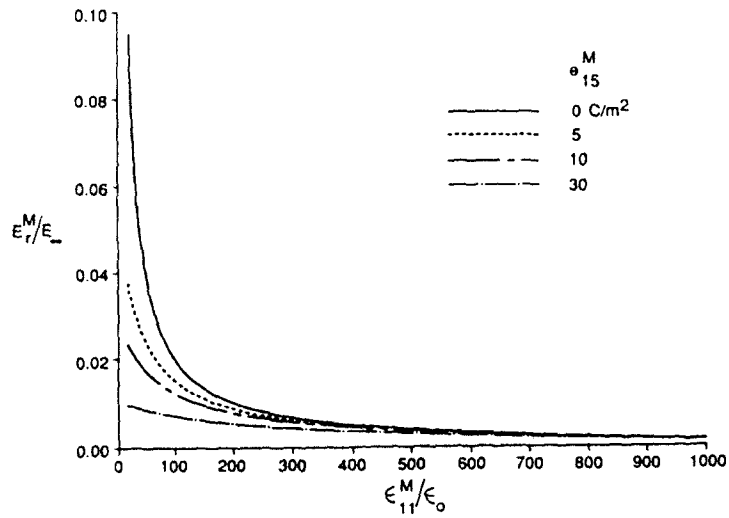

Fig. 3. Vanishing of E_r^M at the boundary as e_{15}^M and ε_{11}^M are independently increased.

inside the inclusion. By taking limits on various parameters in the piezoelectric matrix-inclusion solution, we can study the stress and electric field concentrations for the following cases.

Case 1

Elastic dielectric inclusion ($e_{15}^{I} = 0$) in elastic dielectric matrix ($e_{15}^{M} = 0$). Since there is no piezoelectric coupling in this case, the elastic fields and the electrical fields are decoupled. The maximum shear stress in the matrix at the interface and in the inclusion are

$$\sigma_{z\theta}^{M}(a, 0) = \frac{2c_{44}^{M}}{c_{44}^{M} + c_{44}^{I}}\tau_{\infty}, \quad \sigma_{zr}^{M}(a, \pi/2) = \sigma_{zy}^{I} = \frac{2c_{44}^{I}}{c_{44}^{M} + c_{44}^{I}}\tau_{\infty}. \tag{17}$$

For the case of a hole ($c_{44}^{I} = 0$), we reproduce the elastostatic antiplane shear stress concentration of two at $\theta = 0$. When the matrix is stiffer than the inclusion, $c_{44}^{M} > c_{44}^{I}$, the maximum stress concentration occurs in the matrix at $\theta = 0$. However, when the inclusion is stiffer than the matrix, $c_{44}^{I} > c_{44}^{M}$, the maximum stress concentration occurs at $\theta = \pi/2$ where the shear stress σ_{zr}^{M} in the matrix is equal to the constant shear stress σ_{zy}^{I} of the inclusion. This shifting of the maximum stress location is also observed in the plane strain case (Goodier, 1933). The shear stress σ_{zy} along the lines $\theta = 0$ and $\theta = \pi/2$ are respectively plotted in Figs 4(a, b) as a function of the non-dimensional coordinate r/a for various ratios of the elastic constants c_{44}^{M}/c_{44}^{I}.

Analogously, the electric field concentration in the matrix at the interface and in the inclusion is

$$E_{\theta}^{M}(a, 0) = E_{y}^{I} = \frac{2\varepsilon_{11}^{M}}{\varepsilon_{11}^{M} + \varepsilon_{11}^{I}}E_{\infty}. \tag{18}$$

The electric field concentration in the matrix at $\theta = 0$ as well as inside the inclusion approaches two as the dielectric constant for the matrix becomes much larger than that for the inclusion. A cavity, for example, in a material with high dielectric constant can experience twice the applied electric field. Therefore, arching (dielectric breakdown of air) can occur inside the cavity when subjected to a high electric field during a poling process.

Case 2

Piezoelectric inclusion in elastic matrix ($e_{15}^{M} = 0$, $\varepsilon_{11}^{M} = 0$). Piezoelectric composite sensors are often made in this configuration where a piezoelectric rod is embedded in an elastic matrix (usually polymers). Our interest in this case is to maximize the sensitivity of the sensor, i.e. to maximize the field produced in the piezoelectric inclusion due to the mechanical deformation of the surrounding matrix. The electric field produced inside the piezoelectric inclusion is

$$E_{y}^{I} = -\frac{2e_{15}^{I}}{e_{15}^{I^2} + \varepsilon_{11}^{I}(c_{44}^{M} + c_{44}^{I})}\tau_{\infty}. \tag{19}$$

This expression shows non-monotonic dependence of the induced electric field on e_{15}^{I}. This non-monotonic dependence is plotted in Fig. 5 for various ratios of the elastic constants c_{44}^{M}/c_{44}^{I}. The maximum sensitivity can be achieved by matching the piezoelectric constant of the inclusion to be

$$e_{15}^{I} = \pm\sqrt{\varepsilon_{11}^{I}(c_{44}^{M} + c_{44}^{I})}. \tag{20}$$

This is an interesting phenomenon in that maximizing the piezoelectric constant alone will not necessarily maximize the sensitivity of the sensor; it has to be matched with the rest of the material parameters.

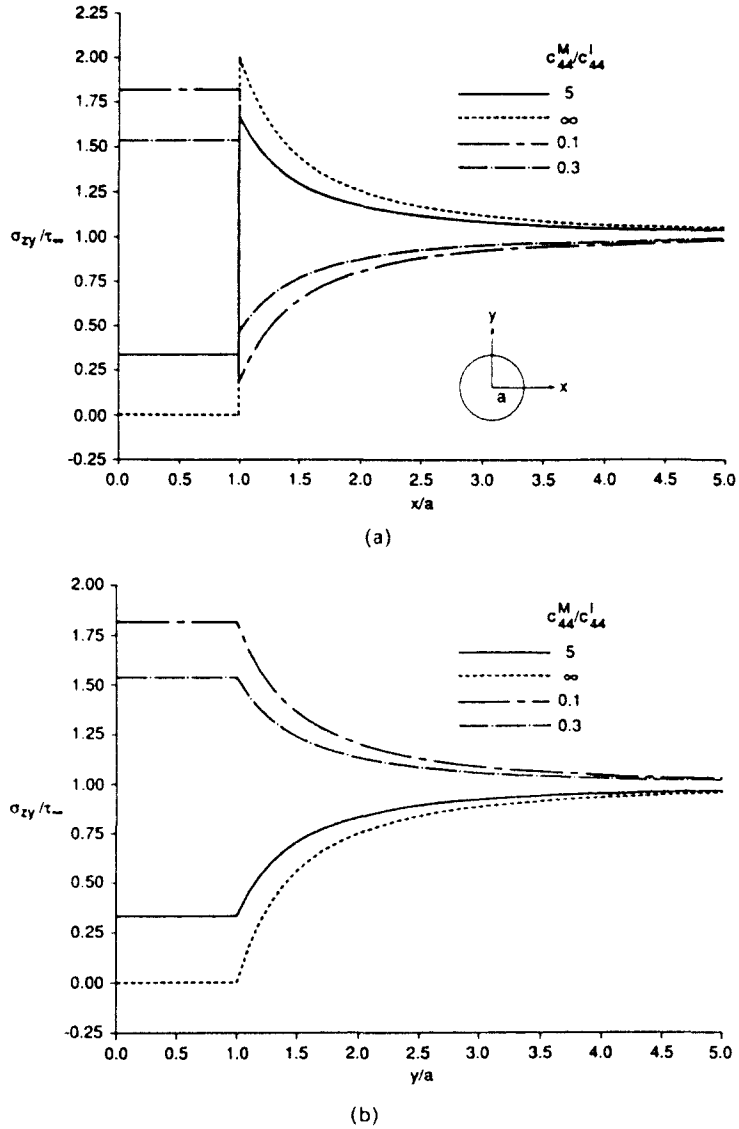

Fig. 4. Plot of σ_{zy} along (a) $\theta = 0$, (b) $\theta = \pi/2$ for purely elastic case.

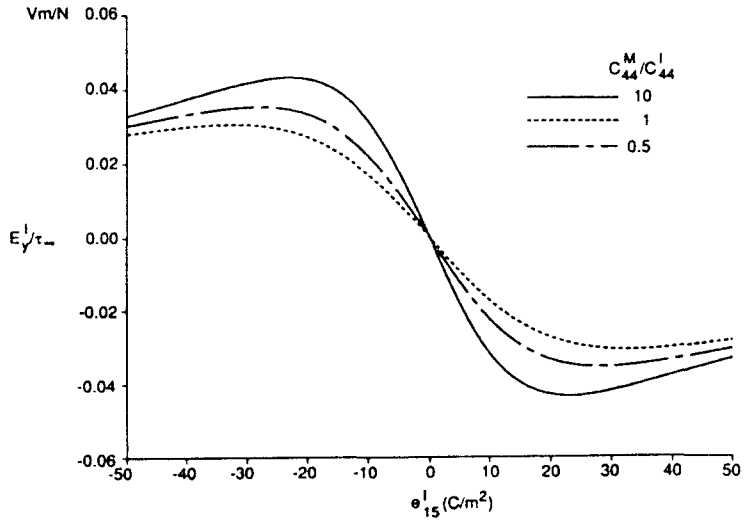

Fig. 5. Non-monotonic dependence of the induced electric field on e^I_{15}.

Case 3

Elastic dielectric inclusion ($e^{I}_{15} = 0$) in piezoelectric matrix. In this case, the inclusion models a non-piezoelectric secondary-phase particle or a fiber in a piezoelectric material. The stress and the electric field concentrations induced by a dielectric inclusion are

$$\sigma^{M}_{z\theta}(a,0) = \frac{2\{\tau_\infty[(c^{M}_{44})^2(\varepsilon^{M}_{11}+\varepsilon^{I}_{11}+(e^{M}_{15})^2(c^{M}_{44}-c^{I}_{44}))]-E_\infty c^{I}_{44}e^{M}_{15}[(e^{M}_{15})^2+c^{M}_{44}\varepsilon^{M}_{11}]\}}{c^{M}_{44}[(c^{M}_{44}+c^{I}_{44})(\varepsilon^{M}_{11}+\varepsilon^{I}_{11})+(e^{M}_{15})^2]}$$

$$E^{M}_{\theta}(a,0) = \frac{2[\tau_\infty c^{I}_{44}e^{M}_{15}+E_\infty(c^{M}_{44}+c^{I}_{44})((e^{M}_{15})^2+c^{M}_{44}\varepsilon^{M}_{11})]}{c^{M}_{44}[(c^{M}_{44}+c^{I}_{44})(\varepsilon^{M}_{11}+\varepsilon^{I}_{11})+(e^{M}_{15})^2]}. \tag{21}$$

These expressions show that the concentration of stress and electric field can be induced independently by the mechanical or the electrical load. For the case of a permeable hole ($c^{I}_{44} = 0$), the stress concentration, $\sigma^{M}_{z\theta}(a,0)/\tau_\infty$, is two, and is independent of the applied electric field. At the same time, the electric field concentration becomes

$$E^{M}_{\theta}(a,0) = \frac{2[(e^{M}_{15})^2+c^{M}_{44}\varepsilon^{M}_{11}]}{c^{M}_{44}(\varepsilon^{M}_{11}+\varepsilon^{I}_{11})+(e^{M}_{15})^2}E_\infty. \tag{22}$$

In the limit of dielectric constant for the matrix becoming much greater than that of the inclusion, $\varepsilon^{M}_{11} \gg \varepsilon^{I}_{11}$, the electric field concentration approaches two just as in Case 1.

Case 4

Piezoelectric inclusion in piezoelectric matrix. In this most general case, the stress and electric field concentration become

$$\sigma^{M}_{z\theta}(a,0) = \left[c^{M}_{44}a_1+e^{M}_{15}c_1+\frac{c^{M}_{44}b_1+e^{M}_{15}d_1}{a^2}\right]$$

$$\sigma^{M}_{zr}(a,\pi/2) = \sigma^{I}_{zy} = \left[c^{M}_{44}a_1+e^{M}_{15}c_1-\frac{c^{M}_{44}b_1+e^{M}_{15}d_1}{a^2}\right]$$

$$E^{M}_{\theta}(a,0) = E^{I}_{y} = -g_1 \tag{23}$$

where a_1, b_1, c_1, d_1 and g_1 are given in eqn (12). It is interesting to note that a uniform stress field results when the elastic constant and the piezoelectric constant are the same for the inclusion and the matrix. However, a uniform electric field results only when all three constants (elastic, dielectric and piezoelectric) are matched. Stress concentrations in the matrix at $\theta = 0$ and $\theta = \pi/2$ with $\tau_\infty = 5\times10^7$ N m^{-2} and $E_\infty = 10^6$, 0, -10^6 V m^{-1} are respectively plotted in Figs 6(a, b) as a function of the ratio of piezoelectric constants, e^{M}_{15}/e^{I}_{15}, while letting $c^{M}_{44} = c^{I}_{44} = 3.53\times10^{10}$ N m^{-2}, $\varepsilon^{M}_{11} = \varepsilon^{I}_{11} = 1.51\times10^{-8}$ C V^{-1} m^{-1} and $e^{I}_{15} = 10.0$ C m^{-2}. The negative electric field implies the reversal of the applied field and the negative piezoelectric constant implies the reversal of the poling direction. As plots indicate, the stress concentration can be greater than two (maximum limit for purely elastic case) when an electric field is applied. In Fig. 7(a), the electric field concentration is plotted as a function of the ratio of dielectric constants for the matrix and the inclusion while holding $c^{M}_{44} = c^{I}_{44} = 3.53\times10^{10}$ N m^{-2}, $e^{M}_{15} = e^{I}_{15} = 17.0$ C m^{-2} and $\varepsilon^{I}_{11} = 1.51\times10^{-8}$ C V^{-1} m^{-1}. It is shown that the mechanical load has no effect on the electric field concentration, which approaches two for a large $\varepsilon^{M}_{11}/\varepsilon^{I}_{11}$ ratio. The effect of the piezoelectric constant on electric field concentration is plotted in Fig. 7(b). Here too it is shown that the electric field concentration can be greater than two (maximum limit for purely electrical case) when a mechanical load is applied.

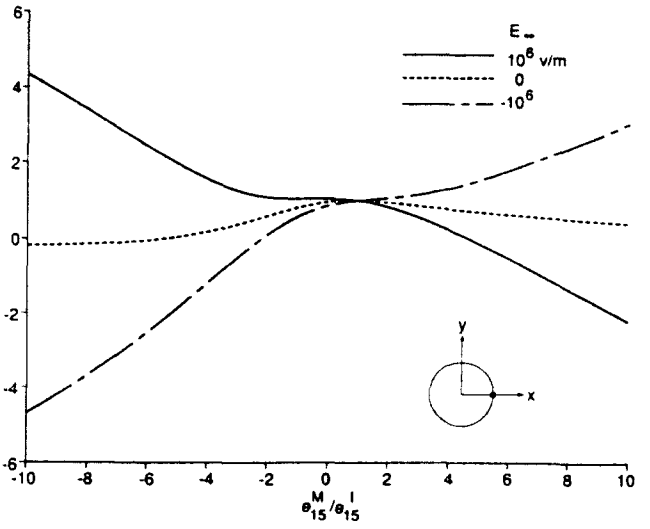

(a)

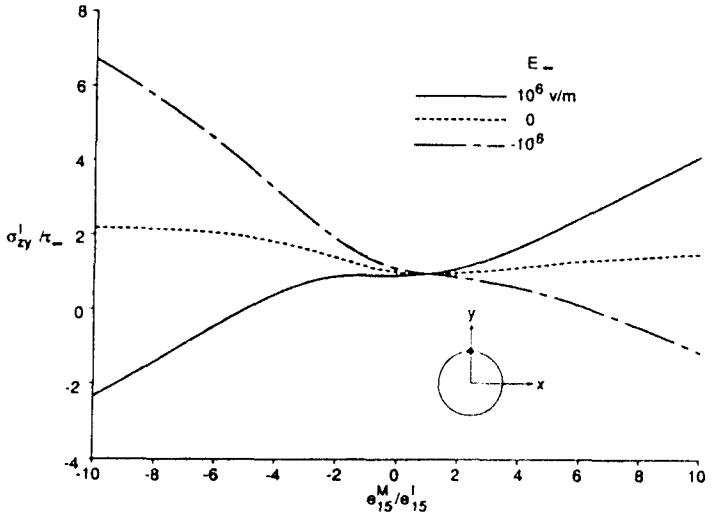

(b)

Fig. 6. Stress concentration at (a) $\theta = 0$, (b) $\theta = \pi/2$ for piezoelectric inclusion in piezoelectric matrix case.

A more interesting phenomenon can be observed, for example, when we let $e_{15}^M = e_{15}^I$ (17.0 C m^{-2}) and $\varepsilon_{11}^M = \varepsilon_{11}^I$ (1.51×10^{-8} C V^{-1} m^{-1}). In this case, the electric field in the matrix at $\theta = 0$ and in the inclusion is

$$E_\theta^M(a,0) = E_y^I = \frac{2[\tau_\infty e_{15}(c_{44}^I - c_{44}^M) + E_\infty(c_{44}^M + c_{44}^I)(e_{15}^2 + c_{44}\varepsilon_{11})]}{c_{44}^M[4e_{15}^2 + 2(c_{44}^M + c_{44}^I)\varepsilon_{11}]}. \tag{24}$$

Figure 8(a) with $c_{44}^I = 3.53 \times 10^{10}$ N m^{-2} shows that the electric field concentration increases dramatically as the shear modulus of the piezoelectric matrix becomes smaller. This is not surprising in examining the expression given in eqn (24), which contains the c_{44}^M term in the denominator.

Similarly, a high electric field concentration behavior can be observed when we let $c_{44}^M = c_{44}^I$ (3.53×10^{10} N m^{-2}), and $\varepsilon_{11}^M = \varepsilon_{11}^I$ (1.51×10^{-8} C V^{-1} m^{-1}). The electric field concentration for this case is

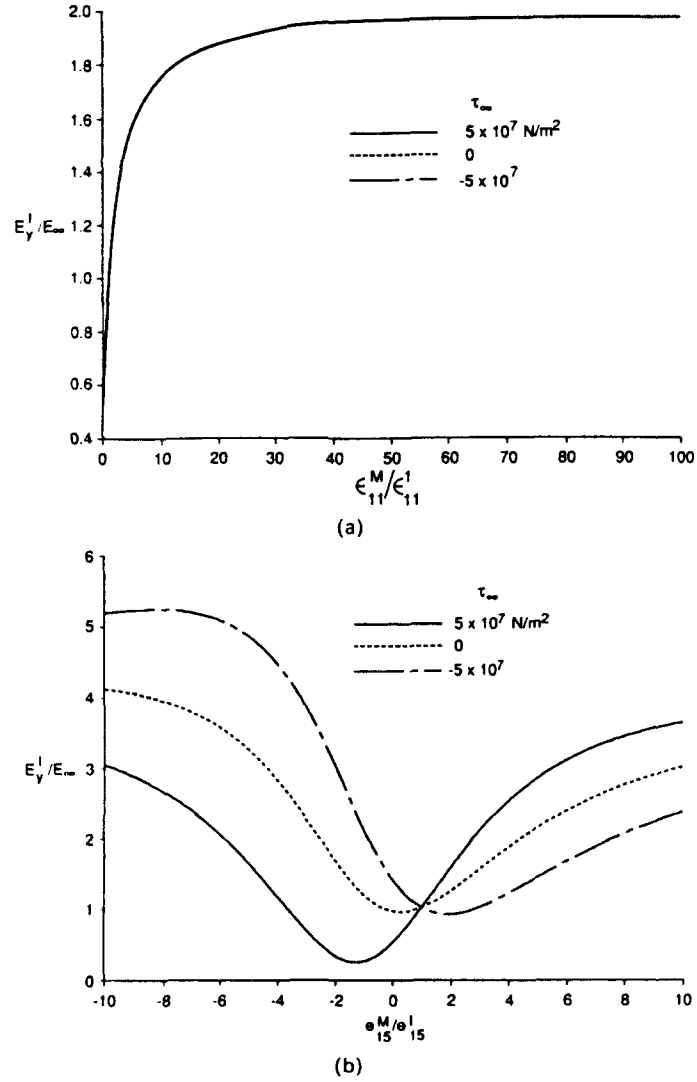

Fig. 7. Electric field concentration as a function of the ratio of (a) dielectric constants, (b) piezoelectric constants.

$$E_\theta^M(a,0) = E_y^I = \frac{2\{\tau_\infty(e_{15}^M - e_{15}^I) + 2E_\infty[(e_{15}^M)^2 + c_{44}\varepsilon_{11}]\}}{(e_{15}^M + e_{15}^I)^2 + 4c_{44}\varepsilon_{11}}. \tag{25}$$

One can maximize the electric field concentration by minimizing the denominator. This can be achieved by letting the magnitude of piezoelectric constants for the inclusion and the matrix be the same but opposite in sign (same material but poled in opposite directions) such that $e_{15}^M + e_{15}^I = 0$. Electric field induced in the inclusion when the mechanical load of $\tau_\infty = -10^6$ N m^{-2} is applied is shown in Fig. 8(b), with $e_{15}^I = 17$ C m^{-2}. Plots show a case where either the elastic constant or the dielectric constant is lowered by a factor of 10, a case where both of them are lowered by a factor of 10, and a case where the piezoelectric constant is increased by a factor of 10. The figure shows high electric field concentration at $e_{15}^M/e_{15}^I = -1$. At this ratio, in the absence of an applied electric field ($E_\infty = 0$), the electric field concentration becomes

$$E_\theta^M(a,0) = E_y^I = -\frac{e_{15}}{c_{44}\varepsilon_{11}}\tau_\infty. \tag{26}$$

This shows that we can increase the induced electric field by decreasing the elastic and

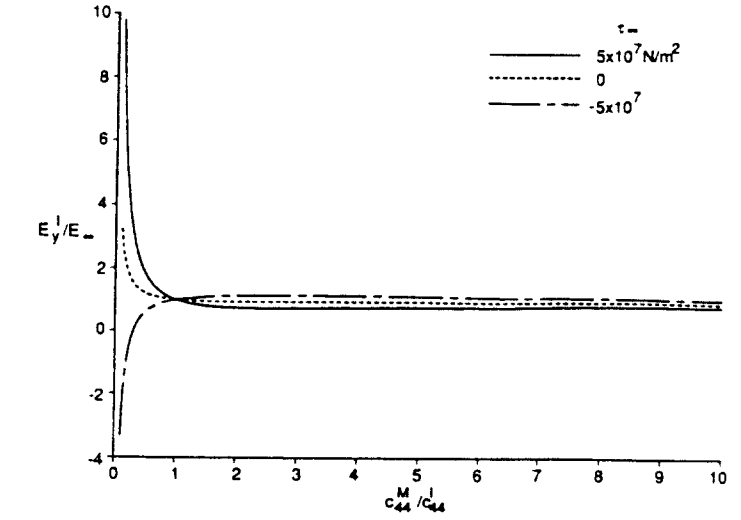

(a)

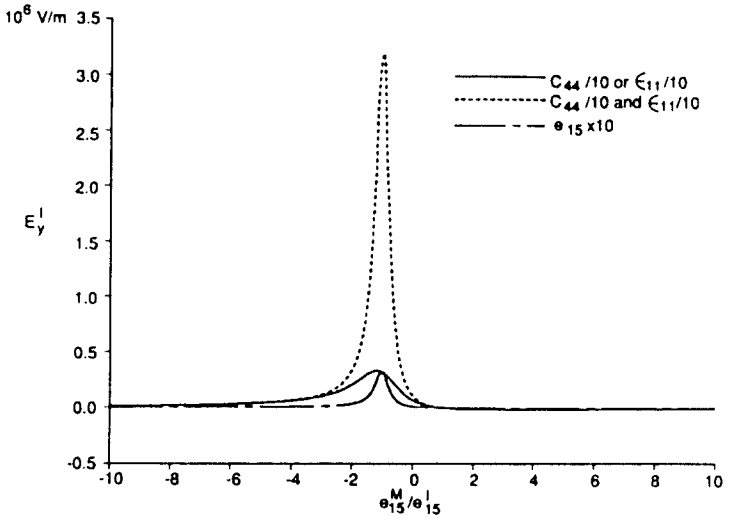

(b)

Fig. 8. High electric field concentration when (a) c_{44}^M/c_{44}^I is small, (b) $e_{15}^M = -e_{15}^I$, and the elastic and the dielectric constants are lowered by an order of magnitude.

dielectric constants and increasing the piezoelectric constant as Fig. 8(b) demonstrates. If we can fabricate piezoelectric materials with lower elastic and dielectric constants but a higher piezoelectric constant than what is currently available, then it is feasible that this phenomenon can be utilized to build a very sensitive sensor. It is to be emphasized that this phenomenon occurs for the piezoelectric matrix–piezoelectric inclusion composite system only when $e_{15}^M = -e_{15}^I$ (matrix and inclusion poled in opposite directions). Solving for E_y and γ_{zy} in terms of σ_{zy} and D_y and letting $D_y = 0$, we can find the electric field induced in a homogeneous piezoelectric material due to a mechanical load:

$$E_y^H = -\frac{e_{15}}{e_{15}^2 + c_{44}\varepsilon_{11}}\tau_\infty. \tag{27}$$

The coefficient multiplying τ_∞ is effectively a g_{15} constant (a piezoelectric constant that relates stress to electric field) that cannot be made arbitrarily large by decreasing c_{44} and ε_{11} because we have the e_{15} term in the denominator. The ratio of the mechanically induced electric fields in an oppositely poled inclusion and a homogeneous piezoelectric material is

$$\frac{E_y^I}{E_y^H} = 1 + \frac{e_{15}^2}{c_{44}\varepsilon_{11}}. \tag{28}$$

Substituting in values for typical piezoceramics, the above expression shows that oppositely poled matrix-inclusion configuration exhibits about 50% higher sensitivity than a homogeneous material.

PATH-INDEPENDENT M-INTEGRAL

The path-independent M-integral, one of the three conservation laws arising in linear elastostatics, was discovered independently by Günther (1962) and Knowles and Sternberg (1972). It was later interpreted by Budiansky and Rice (1973) to be the energy-release rate for a self-similarly expanding defect completely enclosed by the contour of the integral. We can generalize this path-independent integral to include piezoelectric effect by employing a simple method introduced in Eischen and Herrmann (1987). Following their method of taking divergence of the moment of the Lagrangian density (in this case electric enthalpy density h), we obtain

$$\oint_S \left[h x_k n_k - t_i u_{i,k} x_k + D_k n_k E_i x_i - \left(\frac{n-2}{2}\right)(t_k u_k + D_k n_k \phi) \right] \mathrm{d}S, \tag{29}$$

where $n = 2$ for two dimensions and $n = 3$ for three dimensions, $t_i = \sigma_{ij} n_j$ is the traction vector, and n_i is the outer unit normal to the surface S. Evaluating this expression on a contour surrounding the inclusion and taking various limits on the material parameters we obtain the following results.

Case I

Elastic dielectric inclusion in elastic dielectric matrix. By letting $e_{15}^M = e_{15}^I = 0$, we can decouple the mechanical and electrical fields and obtain

$$M = 2\pi a^2 \left[\frac{(c_{44}^M - c_{44}^I)}{c_{44}^M (c_{44}^M + c_{44}^I)} \tau_\infty^2 + \frac{\varepsilon_{11}^M (\varepsilon_{11}^I - \varepsilon_{11}^M)}{(\varepsilon_{11}^M + \varepsilon_{11}^I)} E_\infty^2 \right]. \tag{30}$$

The first term represents the change in the total elastic energy as the inclusion expands self-similarly under the mechanical load. The second term represents the release of the total electrical energy as the inclusion expands self-similarly under the electrical load. For the mechanical case, the energy released is positive when the matrix is stiffer than the inclusion, indicating that the system prefers (the total system energy is lower) to have a bigger inclusion when the inclusion is softer. However, in the electrical case, the system prefers to have a smaller inclusion when the dielectric constant of the matrix is greater than that of the inclusion. This agrees with the well known electrostatics theory that the total electrical energy of the system decreases as the effective dielectric constants increase. This phenomenon is also observed in crack analysis, which showed that the electric field tends to retard the crack growth (Pak, 1990a). This effect can be demonstrated in a simple experiment in which a dielectric slab partially inserted between two charged parallel capacitor plates gets drawn in to fill the remaining gap, increasing the overall effective dielectric constant of the capacitor (Halliday and Resnick, 1966). It is interesting to note that the mechanical energy-release rate is at a maximum when $c_{44}^M = (\sqrt{2}+1)c_{44}^I$, and the electrical energy-release rate is maximum when $\varepsilon_{11}^M = (\sqrt{2}-1)\varepsilon_{11}^I$.

Case 2

Impermeable hole ($c_{44}^{I} = 0$, $e_{15}^{I} = 0$, $\varepsilon_{11}^{I} = 0$) in piezoelectric matrix. Since we have shown that the impermeable boundary condition at the rim of the hole is a good approximation, we can evaluate the M-integral using the solution for an impermeable hole in a piezoelectric matrix. For this case, we obtain

$$M = \frac{2\pi a^2 [\tau_z^2 - E_z^2 [(e_{15}^{M})^2 + c_{44}^{M} \varepsilon_{11}^{M}]]}{c_{44}^{M}}. \tag{31}$$

Again we observe that the electric field effect counteracts the elastic effect and tends to inhibit self-similar growth of the hole. One is reminded that this force is not an actual force acting on the material but rather a generalized thermodynamic force acting on the configurational defect such as a hole. However, it may warrant a further study to see whether this force has a physical manifestation in the surface charges that appear on the rim of the hole, which may have a net attractive force opposing the hole from getting bigger. Using typical values for the material constants with $\tau_z = 5 \times 10^7$ N m^{-2} (maximum tensile strength for some piezoceramics) and $E_z = 10^6$ V m^{-1} (near poling field), the negative electrical term decreases the value of M by about 33%.

Case 3

Piezoelectric inclusion in piezoelectric matrix. In this general case, the M-integral becomes

$$M = 2\pi[a_1(c_{44}^{M} b_1 + e_{15}^{M} d_1) + c_1(e_{15}^{M} b_1 - \varepsilon_{11}^{M} d_1)] \tag{32}$$

where the constants are given in eqn (12). To study the effects of each material parameters on the energy-release rate, the M-integral is plotted in Figs 9(a–c) for the cases of applied mechanical load, electrical load, and both mechanical and electrical loads. The same material constants are used as in the stress and electric field concentration study considered in the previous section. Figures 9(a, c) clearly demonstrate the point that the material prefers to have larger, elastically soft (more compliant) and larger, electrically soft (more polarizable) inclusion.

As should be the case, the value of the M-integral is zero when evaluated on a contour inside the inclusion where all the fields are constant and are independent of the characteristic length a.

CONCLUDING REMARKS

By taking the plane of analysis to be normal to the poling axis of a piezoceramic material, we were able to analyse the piezoelectric antiplane problem in which a circular piezoelectric inclusion embedded in a piezoelectric matrix is subjected to a far-field mechanical and an electrical load. It was shown that both stress and electric field concentration can occur due to the mismatch in the material constants. It was also shown that when an internal cavity problem in piezoelectric materials is analysed, the impermeable boundary condition at the interface between the material and the cavity is a good approximation, provided that the material has strong electro-elastic coupling and high dielectric constants. It was shown that even in the static case, "tuning" of the material constants is required to produce maximum sensitivity for the piezoelectric composite sensor. The phenomena of very high electric field concentration that can be induced by tailoring material parameters is revealed, which can lead to a development of very sensitive sensors. The generalized path-independent M-integral showed that the material favors larger inclusion under the mechanical load when the elastic constant of the inclusion is lower than the matrix. However, in the case of electric field loading, the material favors smaller inclusion when the dielectric constant of the inclusion is less than that of the matrix. These effects may contribute to

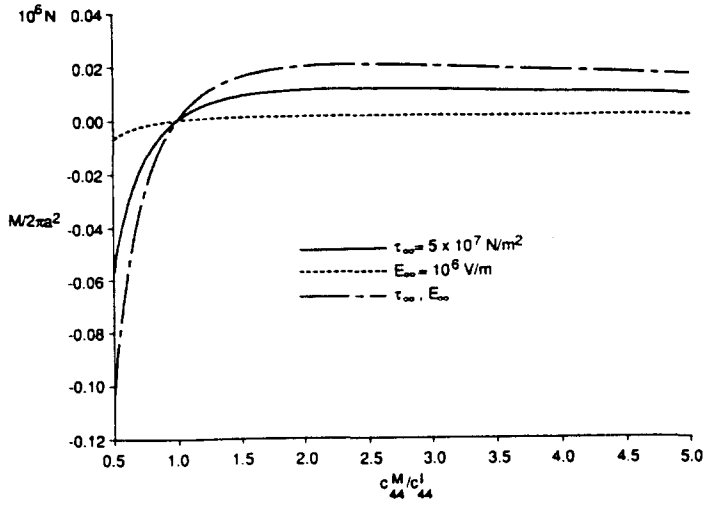

(a)

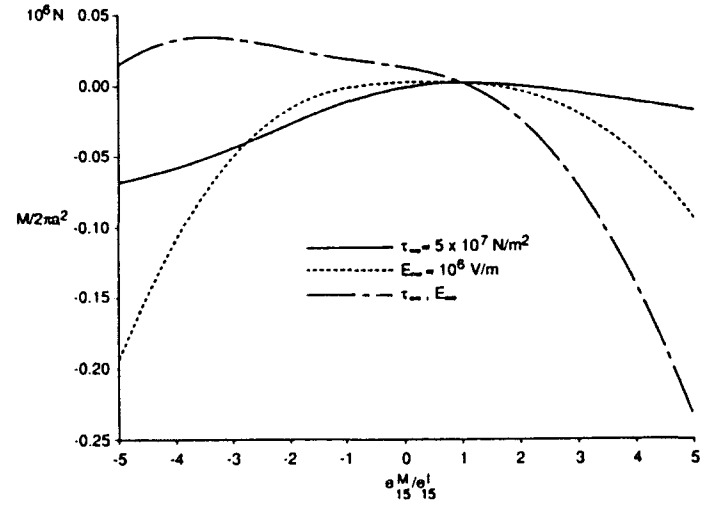

(b)

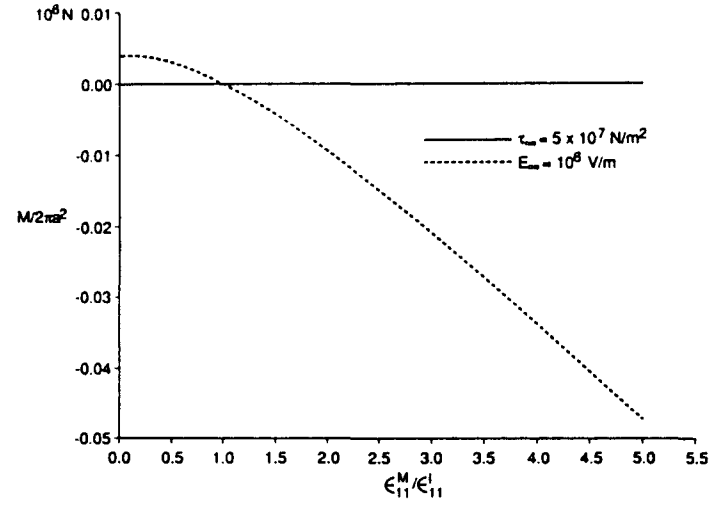

(c)

Fig. 9. Self-similar expansion force as a function of the ratios of (a) elastic constants, (b) piezoelectric constants, (c) dielectric constants.

thermodynamic forces that influence the microstructural evolution and phase transformation in ferroelectric and piezoelectric materials.

Acknowledgements—This work was supported by the Independent Research and Development Program at Grumman Corporate Research Center.

REFERENCES

Berlincourt, D. A., Curran, D. R. and Jaffe, H. (1964). Piezoelectric and piezomagnetic materials and their function in transducers. In *Physical Acoustics* (Edited by W. P. Mason), Vol. 1. Academic Press, New York.
Bleustein, J. L. (1968). New surface wave in piezoelectric materials. *Appl. Phys. Lett.* **13**, 412–413.
Budiansky, B. and Rice, J. R. (1973). Conservation laws and energy release rates. *J. Appl. Mech.* **40**, 201.
Deeg, W. F. (1980). The analysis of dislocation, crack, and inclusion problems in piezoelectric solids. Ph.D. Thesis, Stanford University.
Eischen, J. W. and Herrmann, G. (1987). Energy release rates and related balance laws in linear elastic defect mechanics. *J. Appl. Mech.* **54**, 388–392.
Fano, R. M., Chu, L. J. and Adler, R. B. (1960). *Electromagnetic Fields, Energy, and Forces*. Wiley, New York.
Goodier, J. N. (1933). Concentration of stress around spherical and cylindrical inclusions and flaws. *Trans. ASME* **55**, 39.
Günther, W. (1962). Über einige Randintegrale der Elastomechanik. *Abhandlungen der Braunschweigischen Wissenschaftlichen Gesellschaft* XIV Verlag Friedr. Vieweg & Sohn, Braunschweig.
Halliday, D. and Resnick, R. (1966). *Physics* II. Wiley, New York.
Honein, T., Honein, B., Honein, E. and Herrmann, G. (1990). On piezoelectric circular inclusions. In *Mechanical Modelling of New Electromagnetic Materials* (Edited by R. K. T. Hsieh), p. 259. Elsevier, Amsterdam, 259.
Knowles, J. K. and Sternberg, E. (1972). On a class of conservation laws in linearized and finite elastostatics. *Arch. Rat. Mech. Anal.* **44**, 187–211.
McMeeking, R. M. (1989). Electrostrictive stresses near crack-like flaws. *J. Appl. Math. Phys. (ZAMP)* **40**, 615–627.
Pak, Y. E. (1990a). Crack extension force in a piezoelectric material. *J. Appl. Mech.* **57**, 647–653.
Pak, Y. E. (1990b). Force on a piezoelectric screw dislocation. *J. Appl. Mech.* **57**, 863–869.
Parton, V. Z. (1976). Fracture mechanics of piezoelectric materials. *Acta Astronautica* **3**, 671–683.
Shindo, Y. and Ozawa, E. (1990). Dynamic analysis of a cracked piezoelectric material. *Mechanical Modelling of New Electromagnetic Materials* (Edited by R. K. T. Hsieh), p. 297. Elsevier, Amsterdam.
Shintani, K. and Minagawa, S. (1988). Fields of displacement and electric potential produced by moving dislocations in anisotropic piezoelectric crystals. *Int. J. Engng Sci.* **26**, 89.
Sosa, H. A. (1991). Plane problems in piezoelectric media with defects. *Int. J. Solids Structures* **28**, 491–505.
Suo, Z. (1991). Mechanics concepts for failure in ferroelectric ceramics. In *Smart Structures and Materials* (Edited by G. K. Haritos and A. V. Srinivasan), ASME AD-Vol. 24 AMD-Vol. 123, pp. 1–6. ASME, New York.
Tiersten, H. F. (1969). *Linear Piezoelectric Plate Vibrations*. Plenum Press, New York.
Wang, B. (1992). Three-dimensional analysis of an ellipsoidal inclusion in a piezoelectric material. *Int. J. Solids Structures* **29**, 293–308.
Zhou, S. A., Hsieh, R. K. T. and Maugin, G. A. (1986). Electric and elastic multipole defects in finite piezoelectric media. *Int. J. Solids Structures* **22**, 1411.

APPENDIX A

Governing equations for a linear elastic piezoelectric material occupying region V bounded by surface S can be derived from the following Hamilton's principle (Tiersten, 1969):

$$\delta \int_V h \, \mathrm{d}V - \int_V (f_i \delta u_i - q_b \delta\phi) \, \mathrm{d}V - \int_S (T_i \delta u_i - q_s \delta\phi) \, \mathrm{d}S = 0, \tag{A1}$$

where f_i is the body force, u_i is the displacement, q_b is the body charge, T_i is the applied surface traction, q_s is the applied surface charge and ϕ is the electric potential whose negative of the gradient is the electric field,

$$E_k = -\phi_{,k}. \tag{A2}$$

For linear elastic piezoelectric materials, the electric enthalpy density is expressed as

$$h(\varepsilon_{ij}, E_i) = \tfrac{1}{2} C_{ijkl} s_{ij} s_{kl} - \tfrac{1}{2} \varepsilon_{ij} E_i E_j - e_{ikl} s_{kl} E_i, \tag{A3}$$

where C_{ijkl} are the elastic moduli measured in a constant electric field, ε_{ij} are the dielectric constants measured at constant strain, e_{ikl} are the piezoelectric constants, and s_{ij} is the strain tensor,

$$s_{ij} = \tfrac{1}{2}(u_{i,j} + u_{j,i}). \tag{A4}$$

The variational formulation provides the following results:

Governing field equations,

$$\sigma_{ij,j}+f_i=0 \quad D_{i,i}=q_b, \tag{A5}$$

boundary conditions,

$$\sigma_{ij}n_j=T_i \quad D_in_i=-q_s, \tag{A6}$$

and constitutive equations,

$$\sigma_{ij}=\frac{\partial h}{\partial \varepsilon_{ij}}=C_{ijkl}s_{kl}-e_{kij}E_k, \quad D_i=-\frac{\partial h}{\partial E_i}=e_{ikl}s_{kl}+\varepsilon_{ik}E_k, \tag{A7}$$

where n_i is the outer unit normal vector to S.

APPENDIX B

The constitutive relations for poled piezoelectric ceramic with x_z as the poling axis are of the form (Berlincourt *et al.*, 1964):

$$\begin{Bmatrix}\sigma_{xx}\\ \sigma_{yy}\\ \sigma_{zz}\\ \sigma_{zy}\\ \sigma_{zx}\\ \sigma_{xy}\end{Bmatrix}=\begin{bmatrix}c_{11}&c_{12}&c_{13}&0&0&0\\ c_{12}&c_{11}&c_{13}&0&0&0\\ c_{13}&c_{13}&c_{33}&0&0&0\\ 0&0&0&c_{44}&0&0\\ 0&0&0&0&c_{44}&0\\ 0&0&0&0&0&\frac{1}{2}(c_{11}-c_{12})\end{bmatrix}\begin{Bmatrix}s_{xx}\\ s_{yy}\\ s_{zz}\\ 2s_{zy}\\ 2s_{zx}\\ 2s_{xy}\end{Bmatrix}-\begin{bmatrix}0&0&e_{31}\\ 0&0&e_{31}\\ 0&0&e_{33}\\ 0&e_{15}&0\\ e_{15}&0&0\\ 0&0&0\end{bmatrix}\begin{Bmatrix}E_x\\ E_y\\ E_z\end{Bmatrix} \tag{B1}$$

$$\begin{Bmatrix}D_x\\ D_y\\ D_z\end{Bmatrix}=\begin{bmatrix}0&0&0&0&e_{15}&0\\ 0&0&0&e_{15}&0&0\\ e_{31}&e_{31}&e_{33}&0&0&0\end{bmatrix}\begin{Bmatrix}\varepsilon_{xx}\\ \varepsilon_{yy}\\ \varepsilon_{zz}\\ 2\varepsilon_{zy}\\ 2\varepsilon_{zx}\\ 2\varepsilon_{xy}\end{Bmatrix}+\begin{bmatrix}\varepsilon_{11}&0&0\\ 0&\varepsilon_{11}&0\\ 0&0&\varepsilon_{33}\end{bmatrix}\begin{Bmatrix}E_x\\ E_y\\ E_z\end{Bmatrix}. \tag{B2}$$

APPENDIX C

Material properties for PZT-5H ceramic (Deeg, 1980).

$$c_{11}=12.6\times10^{10}\,\mathrm{N\,m^{-2}},\quad c_{12}=5.5\times10^{10}\,\mathrm{N\,m^{-2}},\quad c_{13}=5.3\times10^{10}\,\mathrm{N\,m^{-2}},\quad c_{33}=11.7\times10^{10}\,\mathrm{N\,m^{-2}}$$
$$c_{44}=3.53\times10^{10}\,\mathrm{N\,m^{-2}},\quad e_{31}=-6.5\,\mathrm{C\,m^{-2}},\quad e_{33}=23.3\,\mathrm{C\,m^{-2}},\quad e_{15}=17.0\,\mathrm{C\,m^{-2}}$$
$$\varepsilon_{11}=1.51\times10^{-8}\,\mathrm{C\,V^{-1}\,m^{-1}},\quad \varepsilon_{33}=1.30\times10^{-8}\,\mathrm{C\,V^{-1}\,m^{-1}}.$$

Permittivity of free space:

$$\varepsilon_0=8.85\times10^{-12}\,\mathrm{C\,V^{-1}\,m^{-1}}.$$